

Nuclear magnetic resonance and nuclear spin relaxation in AlAs quantum well probed by ESR

A. V. Shchepetilnikov¹, D. D. Frolov¹, Yu. A. Nefyodov¹, I. V. Kukushkin¹,
D. S. Smirnov², L. Tiemann³, C. Reichl³, W. Dietsche³, and W. Wegscheider³

¹*Institute of Solid State Physics RAS, 142432 Chernogolovka, Moscow district, Russia*

²*Ioffe Institute, 194021 St. Petersburg, Russia*

³*Solid State Physics Laboratory, ETH Zurich, Schafmattstrasse 16, 8093 Zurich, Switzerland*

The study of nuclear magnetic resonance and nuclear spin-lattice relaxation was conducted in an asymmetrically doped to $n \sim 1.8 \times 10^{11} \text{ cm}^{-2}$ 16 nm AlAs quantum well grown in the [001]-direction. Dynamic polarization of nuclear spins due to the hyperfine interaction resulted in the so-called Overhauser shift of the two-dimensional conduction electron spin resonance. The maximum shifts achieved in the experiments are several orders of magnitude smaller than in GaAs-based heterostructures indicating that hyperfine interaction is weak. The nuclear spin-lattice relaxation time extracted from the decay of Overhauser shift over time turned out to depend on the filling factor of the two-dimensional electron system. This observation indicates that nuclear spin-lattice relaxation is mostly due to the interaction between electron and nuclear spins. Overhauser shift diminishes resonantly when the RF-radiation of certain frequencies was applied to the sample. This effect served as an indirect, yet powerful method for nuclear magnetic resonance detection: NMR quadrupole splitting of ⁷⁵As nuclei was clearly resolved. Theoretical calculations performed describe well these experimental findings.

Extensive studies of nuclear spin physics in various semiconductor heterostructures have been performed in the past several decades [1–19]. Such keen interest was brought about in view of both applied and fundamental significance of the topic. Nuclear spins may be utilized to store information [10, 20] in terms of spin-based electronics [21–25], as non-equilibrium spin polarization of lattice nuclei may have extremely long lifetime [2]. On the other hand, fundamental properties of the two-dimensional conduction electrons and nuclear spins are interconnected. The effect of huge longitudinal resistance near certain fractional fillings [8, 26] may be mentioned as one of the brightest examples. Moreover, the ground state spin polarization of the two-dimensional electron system (2DES) can be extracted from the Knight shift [27] of the nuclear magnetic resonance (NMR) [3, 4, 9, 12, 14]. This offers the approach to investigate various 2DES exotic states including Wigner crystal [18] and $\nu = 5/2$ state [15–17].

One of the most fruitful approaches is to access nuclear spins experimentally through the spins of conduction electrons coupled to them by the hyperfine interaction. Spin properties of the electrons, in turn, can be effectively studied with the aid of electron spin resonance (ESR). One of the earliest adaptations of this principle for the experiments on GaAs-based heterostructures can be found in the papers [1, 2]. Let us address the idea of studying nuclear spins through ESR in more details. The actual magnetic field position of ESR turned out to be dependent on the spin polarization of the nuclear system. Indeed the spin part of the Hamiltonian for the single electron in a [001] quantum well can be expressed as:

$$H = g^* \mu_B B S_z + \mathbf{I} \hat{A} \mathbf{S} \quad (1)$$

Here g^* is the bare electron g -factor, which does not

take into account the electron-electron exchange interaction [28, 29], μ_B is the Bohr magneton, B is the amplitude of the magnetic field, which is applied along $z \parallel [001]$, $\mathbf{S} = (S_x, S_y, S_z)$ is the spin of an electron, $\mathbf{I} = (I_x, I_y, I_z)$ is the total nuclear spin, and \hat{A} is the hyperfine interaction tensor. Provided the total nuclear spin polarization is non-zero the electron spin splitting ΔE in the structure under study can be presented as

$$\Delta E = g^* \mu_b S_z \left(B + \frac{A_{zz} I_z}{g^* \mu_B} \right) = g^* \mu_b S_z (B + \Delta B) \quad (2)$$

The term $\Delta B = A_{zz} I_z / (g^* \mu_B)$ represents the Overhauser shift [30] of the ESR actual magnetic field position. Under typical experimental conditions thermal energy is several orders of magnitude larger than nuclear spin splitting and nuclear spins are unpolarized, hence, Overhauser shift equals zero. When the electron system is in ESR, nuclear spins become partially polarized as part of the non-equilibrium spin polarization is transferred from the electrons to the nuclear subsystem via hyperfine interaction. By adjusting the external magnetic field so that the resonance conditions for ESR are fulfilled at a rather long period of time it is possible to significantly polarize the nuclear subsystem and to achieve large Overhauser shifts [1, 2]. This process is traditionally referred to as dynamic nuclear polarization.

Now the approach for studying nuclear spin subsystem through ESR becomes obvious. As the Overhauser shift is proportional to the total spin of the nuclei, the rate of the nuclear spin relaxation is exactly the decay rate of this shift, and thus the nuclear spin lattice relaxation rate can be accessed experimentally [2, 31, 32]. Resonant depolarization of nuclear spins will result in resonant diminishing of Overhauser shift allowing the effective NMR detection [1].

In the present paper we report ESR studies of nuclear spins in close proximity to 2DES formed in the AlAs-quantum well. Such a semiconductor heterostructure boasts several peculiar properties. First of all, nuclear spin lifetime turned out to be quite long (several hours). Moreover, in wide [001] quantum wells (wider than 5 nm) the electrons tend to occupy two in-plane valleys located at the X-points of the Brillouin zone along [100] and [010], while in narrow quantum wells the X valley along [001] has lower energy (see Ref. 33). These valleys are characterized by an anisotropic effective mass [34]: $m_t = 0.2 m_0$ and $m_l = 1.1 m_0$, much heavier than in conventional GaAs heterostructures. As a consequence, the ratio between characteristic Coulomb energy and Fermi energy is by far larger and thus the many particle effects are significantly more pronounced in AlAs quantum wells than in GaAs heterostructures. Finally, the value of conduction electron g-factor is large $g^* \approx 1.98$ (see Ref. 35 and 36), whereas the g-factor in GaAs heterostructures depends strongly on the parameters of the structure and the magnetic field [37] but its absolute value does not exceed 0.44. As a result, in AlAs quantum wells electron spin splitting also exceeds the thermal energy correspondent to the temperature of the experiment, $T = 1.5$ K. This results into large intensity of ESR, hence, allowing for the accurate measurements.

The sample under study was a 16 nm AlAs quantum well epitaxially grown along the [001] direction. The Al concentration in the $\text{Al}_x\text{Ga}_{1-x}\text{As}$ barrier layers was equal to 46%. The structure was asymmetrically delta-doped with Si to result in a low temperature sheet density of $n \approx 1.8 \times 10^{11} \text{ cm}^{-2}$. The electron mobility was equal to $\mu = 2 \times 10^5 \text{ cm}^2/\text{V s}$ at the temperature of 1.5 K. Standard indium contacts to the 2D electron system were formed in the common Hall bar geometry. Low temperature characterization of this exact sample can be found in our previous publication [36].

The conventional method of ESR detection in 2DES is based on the sensitivity of the system longitudinal magnetoresistance $R_{xx}(B)$ to the spin resonance in the quantum Hall regime [38]. The ESR is detectable as a sharp peak in $R_{xx}(B)$ magnetic field dependence at a fixed microwave frequency. We have successfully applied this approach to carefully investigate the g-factor anisotropy in GaAs - based heterostructures [39, 40].

An ac probe current of $1 \mu\text{A}$ at the frequency of $\sim 1 \text{ kHz}$ was applied from source to drain. A lock-in amplifier monitored the channel resistance R_{xx} through two sense contacts along the channel. The sample was irradiated by 100% amplitude modulated radiation at a frequency of $f_{mod} \sim 30 \text{ Hz}$; microwave power was delivered through a rectangular oversized waveguide. A number of microwave radiation sources were utilized: generators with frequency multipliers coupled to them, backward wave oscillators - so that we were able to vary the microwave radiation frequency up to 260 GHz. The power of the microwave radiation injected into the waveguide did not exceed 10 mW. A second lock-in amplifier, synchronized

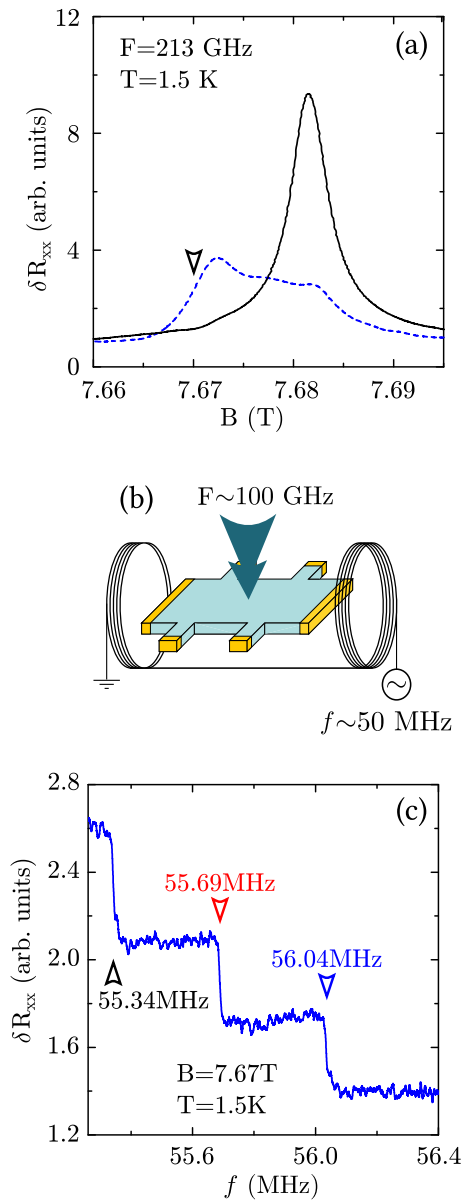


FIG. 1. (a) Typical ESR lineshapes observed in the experiment. Solid line corresponds to the initial ESR, dashed line denotes the ESR peak after dynamical nuclear polarization. A mark denotes the fixed value of magnetic field for the NMR experiment. (b) Schematic of NMR experimental setup. A coil coupled to an RF-source is placed around the sample. The microwave $F \sim 100 \text{ GHz}$ (via waveguide) and radio frequency $f \sim 50 \text{ MHz}$ (via coil) radiation can be applied to the sample. (c) Typical magnetoresistance in the NMR experiment. The steps correspond to three NMR frequencies of ^{75}As (nuclear spin $I = 3/2$) split by quadrupole interaction.

at f_{mod} frequency, was connected to the output of the first one and, thus, measured the variation δR_{xx} in the magnetoresistance, caused by microwave irradiation. Experiments were carried out at the temperature of 1.5 K in the magnetic field up to 10 T.

No traces of dynamic nuclear polarization were ob-

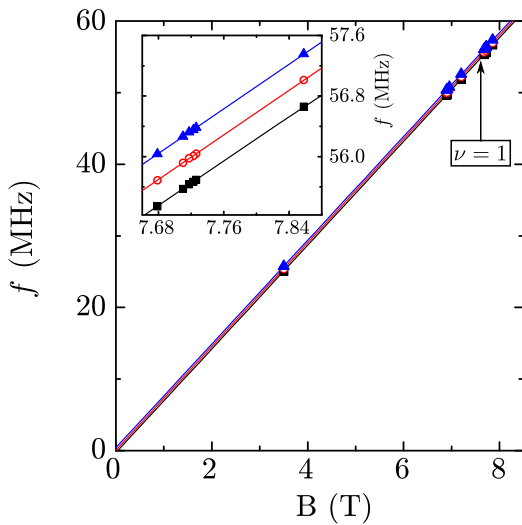


FIG. 2. The dependence of three NMR frequencies on the magnetic field. The inset shows the region of magnetic fields near unity filling factor in more detail.

served in our previous ESR studies [36] of AlAs quantum well. As the rates of the magnetic field sweeps were high, the electron spins remained in resonance for only limited periods of time and, as a consequence, the amount of angular momentum transferred to the nuclear subsystem was negligible. In order to form substantial nuclear spin polarization and to achieve large Overhauser shifts the following procedure was implemented during present work. The microwave resonance frequency was kept constant. The magnetic field was ramped to the exact ESR position. The gradually building up nuclear spin polarization shifted ESR towards lower fields and the magnetic field was then constantly adjusted so that the resonant conditions for ESR were fulfilled for a long period of time. Typically, it took several hours to achieve substantial Overhauser shifts under our experimental conditions. Panel (a) of the Fig. 1 depicts typical ESR lineshapes with (dashed line) and without ESR induced nuclear spin polarization (solid line) measured near unity filling at 1.5 K. The Overhauser shift of about 10 mT is clearly resolved. We were not able to achieve Overhauser shifts larger than 40 mT, the value several orders of magnitude smaller than the one observed in conventional GaAs-heterostructures [7]. According to the Eq. 2 this effect stems from the relative weakness of hyperfine interaction in AlAs and large effective electron g -factor. Another important difference was the ESR lineshape in presence of nuclear spin polarization: in GaAs-based samples ESR shifts as a whole [1], whereas in our experiments ESR splits into separate peaks. The right-most peak retains the initial position, while the left-most one is shifted towards lower magnetic fields.

The nuclear origin of the observed shift was proved by NMR experiments. NMR also allowed us to identify the isotope participating in the dynamic nuclear polarization. For NMR studies a coil coupled to an RF-source

was placed around the sample, so that both the microwave ~ 100 GHz (via waveguide) and radio frequency ~ 50 MHz (via coil) radiation could be applied to the sample. The schematic illustration of the experimental setup is presented in panel (b) of the Fig. 1. The NMR procedure was as follows. The microwave frequency was kept constant and Overhauser shifts large enough to split ESR into well-resolved peaks were achieved (see panel (a) of the Fig. 1). Then the magnetic field was fixed at the position of the lower (in the magnetic field) side of the ESR peak experiencing Overhauser shift (the correspondent magnetic field is indicated by the arrow in panel (a) of the Fig. 1) and then the sweep of the RF-radiation frequency was performed. Near NMR nuclear spins were depolarized and the Overhauser shift resonantly diminished, so that the left-most (on the magnetic field scale) peak moved towards higher fields, as a result, the signal measured by the second lock-in amplifier dropped. Typical signal of the second lock-in amplifier during the RF-radiation frequency sweep is shown in panel (c) of the Fig. 1. Three resonant frequencies resolved are indicated in the panel, the middle one corresponds to the NMR frequency of ^{75}As isotope. No traces of other isotopes including Al and Ga at the corresponding frequencies were found.

The results of the NMR experiments performed near different magnetic fields and filling factors ($\nu = 1$ and $\nu = 2$) are presented in the Fig. 2. Three resonant frequencies were resolved at each magnetic field studied. These frequencies are linear in the magnetic field, whereas differences between the central frequency and two auxiliary ones are equal to each other and remain constant $\delta f = 0.34$ MHz independent of the magnetic field. We attribute this splitting to the quadrupole interaction of arsenic nuclei. The nuclear spin of ^{75}As equals $3/2$, so the magnetic field splits the nuclear spin level into four sublevels with different nuclear momentum projections. Quadrupole interaction modifies the energy separations between these sublevels and during NMR exactly three transitions with different energies become possible resulting into three resonant frequencies of nuclear resonance. Please note, that the quadrupole splitting of the nuclei spins does not depend on the magnetic field. The strength of the splitting can be estimated using the lattice mismatch between the substrate and the quantum well [41], which is about 0.2%. The simplest model calculations [42] yield the quadrupole splitting 0.3 MHz which is in a good agreement with the experimental value.

In order to measure the nuclear spin-lattice relaxation time, τ , non-equilibrium spin polarization of nuclei was first induced with the aid of ESR in the vicinity of unity filling factor at a fixed frequency of 170 GHz. Note, that this whole set of experiments was performed after another cooldown of the sample and thus electron sheet density was slightly different $n \approx 1.5 \times 10^{11} \text{ cm}^{-2}$. The decay of this polarization with time was measured near different fillings as follows. The ESR peak was measured to probe the Overhauser shift, then the magnetic field was quickly

ramped to the position correspondent to a filling factor of interest, where nuclear spins relaxed for a relatively long period of time. Afterwards the magnetic field was ramped back to the initial position to probe Overhauser shift once again. These steps were repeatedly performed several times. Three consecutive ESR peaks recorded during this procedure for filling factor $\nu = 1.04$ are presented in the panel (a) of the Fig. 3. The slow relaxation of the Overhauser shift with time can be clearly seen. Typical dependencies of the Overhauser shift on time are plotted in panel (b) of the Fig. 3 for three different fillings. All of the measured dependencies were exponential so that the decay time could be extracted.

The nuclear spin relaxation rates measured near different filling factors around $\nu = 1$ are presented in panel (c) of the Fig. 3. The relaxation rate is clearly dependent on the state of the electron system and roughly follows the dependence of DOS at the Fermi level on the filling factor. This fact suggests that the main relaxation channel is based on the hyperfine interaction between electron and nuclear spins. However the spin relaxation mechanisms related to the scattering assisted [2] and phonon assisted [43] spin flips are suppressed by the large spin splitting, low temperature and high quality of the structure. This indicates that some other mechanism might be dominant in this case [42], as e.g. the hyperfine mediated nuclear spin diffusion [44], which does not involve real electron spin transitions and allow for the fast long-range nuclear spin transport.

Typical nuclear relaxation times measured around unity fillings are about 200 minutes long and are of the order of magnitude larger than in conventional GaAs heterostructures [2]. This experimental finding indicates the relatively small strength of hyperfine interaction in AlAs.

In order to calculate hyperfine interaction constant microscopically we have adopted the method outlined in Ref. 45. We have decomposed electron Bloch function in the vicinity of the nuclei into the hydrogen-like s , p , d contributions [46, 47] with the coefficients determined from the DFT calculation [42]. The calculation shows that the hyperfine interaction between the electron spin and the spin of arsenic nuclei in AlAs is suppressed by a factor of ≈ 2 as compared to GaAs. The maximum Overhauser shift is estimated to be 250 mT, while for GaAs it is known to be 3.53 T [48]. Note that the degree of nuclear spin polarization in our experiment is about 16%, which is somewhat larger than in Ref. 2.

The main reasons for the drastic difference of Overhauser fields in AlAs and GaAs are the reduced contribution of s shells to the electron Bloch function in the X point of AlAs Brillouin zone and the large effective g -factor. The main contribution to the hyperfine interaction is given by the arsenic nuclei, while the contribution from aluminum is negligible, in full agreement with the experiment. This is caused by the p type symmetry of Al Bloch function and the shift of electron density from cation to anion. The hyperfine interaction tensor is found to be anisotropic due to the reduced symmetry of the X

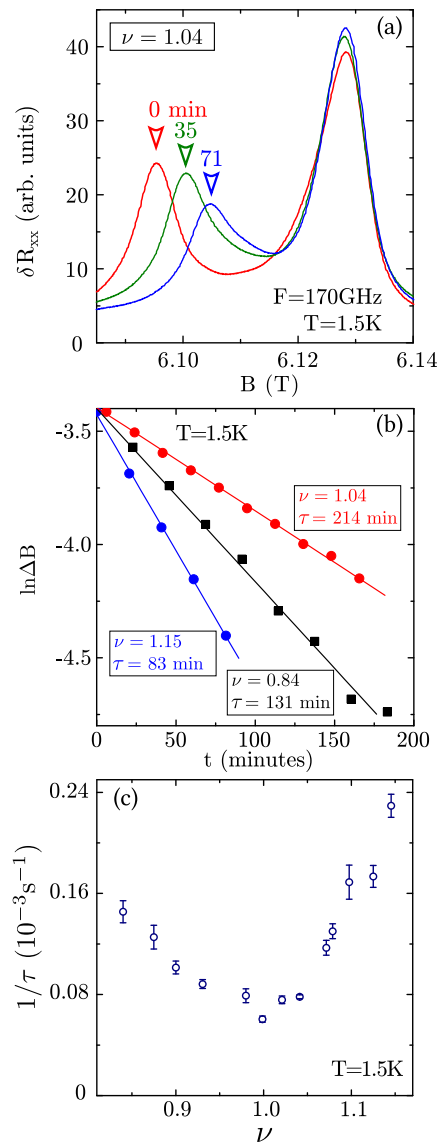


FIG. 3. (a) Three consecutive ESR peaks recorded at different moments of time during the process of nuclear spin relaxation near filling factor $\nu = 1.04$. Elapsed time is indicated near each peak. Initial nuclear spin polarization was achieved with the aid of ESR at a fixed frequency of 170 GHz. (b) The dependencies of the Overhauser shift on time during nuclear spin relaxation near various filling factors $\nu = 0.84, 1.04, 1.15$. The data is fitted with straight lines to extract the characteristic decay time denoted in the panel. (c) The nuclear spin relaxation rate measured near different fillings. The temperature was fixed at 1.5 K throughout the experiment.

valleys in AlAs. Microscopically the main contribution to the hyperfine coupling constant is related with the s shell of As atom and the anisotropy of hyperfine interaction is determined by the contribution of its d shell [42].

To conclude, the Overhauser shift of the two-dimensional conduction electron spin resonance was studied in an asymmetrically doped 16 nm AlAs quantum well grown in the [001]-direction. Non-equilibrium nu-

clear spin polarization was created while the electron system was in ESR, as part of the magnetic momentum was transferred to the nuclear subsystem. The NMR experiments revealed the nuclear isotope participating in dynamic nuclear polarization to be ^{75}As . The NMR was detected by the resonant reduction of Overhauser shift after the RF-radiation of certain frequencies was applied to the sample. The quadrupole splitting of ^{75}As was observed in the NMR experiment. The nuclear spin-lattice relaxation rate was measured by the decay of Overhauser shift over time near different filling factors. The dependence of the relaxation rate on the state of the electron system suggests that the relaxation mechanism is based on the hyperfine interaction between nuclear and electron spins. The maximum Overhauser shifts achieved in the experiments were substantially smaller than in conven-

tional GaAs quantum wells and heterojunctions. This fact suggests that hyperfine interaction is weak in AIs. The microscopical calculations were conducted to prove this statement.

We gratefully acknowledge the financial support of the ESR measurements from Russian Science Foundation (Grant No. 14-12-00693) and cryogenic NMR setup development from Russian Foundation for Basic Research (Grant No. 16-32-00399). D. S. S. is grateful to M. O. Nestoklon and M. M. Glazov for fruitful discussions and acknowledges partial support from the Russian Science Foundation (No. 14-12-501067), RF President Grant No. SP-643.2015.5, Dynasty Foundation, and St.-Petersburg Government Grant. L.T., C.R., W.D. and W.W. acknowledge the financial support from Swiss National Foundation (Quantum Science and Technology).

-
- [1] M. Dobers, K. v. Klitzing, J. Schneider, G. Weimann, and K. Ploog, *Phys. Rev. Lett.* **61**, 1650 (1988).
- [2] A. Berg, M. Dobers, P. R. Gerhardt, and K. von Klitzing, *Phys. Rev. Lett.* **64**, 2563 (1990).
- [3] S. E. Barrett, G. Dabbagh, L. N. Pfeiffer, K. W. West, and R. Tycko, *Phys. Rev. Lett.* **74**, 5112 (1995).
- [4] R. Tycko, S. E. Barrett, G. Dabbagh, L. N. Pfeiffer, and K. W. West, *Science* **268** 1460 (1995).
- [5] P. Khandelwal, N. N. Kuzma, S. E. Barrett, L. N. Pfeiffer, and K. W. West, *Phys. Rev. Lett.* **81**, 673 (1998).
- [6] N. N. Kuzma, P. Khandelwal, S. E. Barrett, N. Pfeiffer, and K. W. West, *Science*, **281**, 686 (1998).
- [7] I. V. Kukushkin, K. v. Klitzing, and K. Eberl, *Phys. Rev. B* **60**, 2554 (1999).
- [8] S. Kronmüller, W. Dietsche, K. v. Klitzing, G. Denninger, W. Wegscheider, and M. Bichler, *Phys. Rev. Lett.* **82**, 4070 (1999).
- [9] S. Melinte, N. Freytag, M. Horvatic, C. Berthier, L. P. Levy, V. Bayot, and M. Shayegan, *Phys. Rev. Lett.* **84**, 354 (2000).
- [10] J. H. Smet, R. A. Deutschmann, F. Ertl, W. Wegscheider, G. Abstreiter and K. von Klitzing, *Nature* **415**, 281 (2002).
- [11] K. Hashimoto, K. Muraki, T. Saku, and Y. Hirayama, *Phys. Rev. Lett.* **88**, 176601 (2002).
- [12] O. Stern, N. Freytag, A. Fay, W. Dietsche, J. H. Smet, K. von Klitzing, D. Schuh, and W. Wegscheider *Phys. Rev. B* **70**, 075318 (2004).
- [13] N. Kumada, K. Muraki, K. Hashimoto, and Y. Hirayama, *Phys. Rev. Lett.* **94**, 096802 (2005).
- [14] N. Kumada, K. Muraki, and Y. Hirayama, *Phys. Rev. Lett.* **99**, 076805 (2007).
- [15] L. Tiemann, G. Gamez, N. Kumada, and K. Muraki, *Science* **335**, 828 (2012).
- [16] M. Stern, B. A. Piot, Y. Vardi, V. Umansky, P. Plochocka, D. K. Maude, and I. Bar-Joseph *Phys. Rev. Lett.* **108**, 066810 (2012).
- [17] B. Friess, V. Umansky, L. Tiemann, K. von Klitzing, and J. H. Smet, *Phys. Rev. Lett.* **113**, 076803 (2014).
- [18] L. Tiemann, T. D. Rhone, N. Shibata, and K. Muraki, *Nature Physics* **10**, 648 (2014).
- [19] T. D. Rhone, L. Tiemann, and K. Muraki, *Phys. Rev. B* **92**, 041301(R)(2015).
- [20] V. Privman, D. Mozysky, I. D. Vagner, *Computer Physics Communications* **146**, 331 (2002).
- [21] S. Datta and B. Das, *Appl. Phys. Lett.* **56** 665 (1990).
- [22] S. A. Wolf, D. D. Awschalom, R. A. Buhrman, J. M. Daughton, S. von Molnár, M. L. Roukes, A. Y. Chtchelkanova, and D. M. Treger, *Science* **294**, 1488 (2001).
- [23] D. D. Awschalom, M. E. Flatté, and N. Samarth, *Sci. Am. (Int. Ed.)* **286**, 66 (2002).
- [24] I. Zutic, J. Fabian, and S. Das Sarma, *Rev. Mod. Phys.* **76** 323 (2004).
- [25] S. D. Bader and S. S. P. Parkin *Annual Review of Condensed Matter Physics* **1**, 71 (2010).
- [26] S. Kronmüller, W. Dietsche, J. Weis, K. von Klitzing, W. Wegscheider, and M. Bichler *Phys. Rev. Lett.* **81**, 2526 (1998).
- [27] W. D. Knight, *Phys. Rev.* **76**, 1259 (1949).
- [28] T. Ando, A. B. Fowler, and F. Stern, *Rev. Mod. Phys.* **54**, 437 (1982).
- [29] Y. P. Shkolnikov, E. P. De Poortere, E. Tutuc, and M. Shayegan, *Phys. Rev. Lett.* **89**, 226805 (2002).
- [30] A. W. Overhauser *Phys. Rev.* **92**, 411 (1953).
- [31] I. I. Ryzhov, S. V. Poltavtsev, K. V. Kavokin, M. M. Glazov, G. G. Kozlov, M. Vladimirova, D. Scalbert, S. Cronenberger, A. V. Kavokin, A. Lemaître, J. Bloch, and V. S. Zapasskii, *Appl. Phys. Lett.* **106**, 242405 (2015).
- [32] I. I. Ryzhov, G. G. Kozlov, D. S. Smirnov, M. M. Glazov, Y. P. Efimov, S. A. Eliseev, V. A. Lovtcius, V. V. Petrov, K. V. Kavokin, A. V. Kavokin, and V. S. Zapasskii, *Sci. Rep.* **6**, 21062 (2016).
- [33] M. Shayegan, E. P. De Poortere, O. Gunawan, Y. P. Shkolnikov, E. Tutuc, and K. Vakili, *Phys. Stat. Sol. (b)* **243**, 3629 (2006).
- [34] V. M. Muravev, A. R. Khisameeva, V. N. Belyanin, I. V. Kukushkin, L. Tiemann, C. Reichl, W. Dietsche, and W. Wegscheider *Phys. Rev. B* **92**, 041303(R) (2015).
- [35] M. Schulte, J. G. S. Lok, G. Denninger and W. Dietsche, *Phys. Rev. Lett.* **94**, 137601 (2005).
- [36] A. V. Shchepetilnikov, Yu. A. Nefyodov, I. V. Kukushkin, L. Tiemann, C. Reichl, W. Dietsche, and W. Wegschei-

- der, Phys. Rev. B **92**, 161301(R) (2015).
- [37] A. V. Shchepetilnikov, Yu. A. Nefyodov, I. V. Kukushkin, and W. Dietsche, J. Phys.: Conf. Ser. **456**, 012035 (2013)
- [38] D. Stein, K.v. Klitzing and G. Weimann, Phys. Rev. Lett. **51**, 130 (1983).
- [39] Yu. A. Nefyodov, A. V. Shchepetilnikov, I. V. Kukushkin, W. Dietsche, and S. Schmult, Phys. Rev. B **83**, 041307(R) (2011).
- [40] Yu. A. Nefyodov, A. V. Shchepetilnikov, I. V. Kukushkin, W. Dietsche, and S. Schmult., Phys. Rev. B **84**, 233302 (2011).
- [41] R. I. Dzhioev and V. L. Korenev, Phys. Rev. Lett. **99**, 037401 (2007).
- [42] See Supplemental Material in the next page.
- [43] J. H. Kim, I. D. Vagner, and L. Xing, Phys. Rev. B **49**, 16777 (1994).
- [44] C. Latta, A. Srivastava, and A. Imamoglu, Phys. Rev. Lett. **107**, 167401 (2011).
- [45] E. I. Gryncharova and V. I. Perel, Semiconductors **11**, 997 (1977).
- [46] J. Fischer, W. A. Coish, D. V. Bulaev, and D. Loss, Phys. Rev. B **78**, 155329 (2008).
- [47] E. Chekhovich, M. Glazov, A. Krysa, M. Hopkinson, P. Senellart, A. Lemaitre, M. Skolnick, and A. Tartakovskii, Nature Physics **9**, 74 (2013).
- [48] B. Urbaszek, X. Marie, T. Amand, O. Krebs, P. Voisin, P. Maletinsky, A. Högele, and A. Imamoglu, Rev. Mod. Phys. **85**, 79 (2013).

Supplemental Material to “Nuclear magnetic resonance and nuclear spin relaxation in AlAs quantum well probed by ESR”

I. S1. QUADRUPOLE SPLITTING ESTIMATION

In GaAs/AlAs heterostructures there is a lattice mismatch $\varepsilon \sim 0.2\%$ at low temperatures, which can be used to roughly estimate the strain in the QW. The strain produces build-in electric fields in the structure. The nuclear quadrupole moments interact with the electric field gradients, which leads to the quadrupole splitting of the nuclear spin states, as described by the Hamiltonian

$$\mathcal{H}_Q = \frac{Q}{2} \left(I_z^2 - \frac{I(I+1)}{3} \right). \quad (\text{S1})$$

In the simplest model [S1] the quadrupole splitting is determined by

$$Q = \frac{3eQS\varepsilon}{2I(2I-1)}, \quad (\text{S2})$$

where Q is the nuclear quadrupole moment and S relates the elastic strains to the electric field gradients. For the arsenic nuclei $Q = 3.1 \cdot 10^{-25} \text{ cm}^2$ and one can use $S = 13.2 \cdot 10^{15} \text{ esu/cm}^3$ measured in GaAs for arsenic nuclei [S2]. Estimation with these values gives the splitting between nuclear spin resonances equal to $Q \approx 0.3 \text{ MHz}$ in surprisingly good agreement with the experimental value.

II. S2. MICROSCOPIC CALCULATION OF HYPERFINE INTERACTION

The hyperfine interaction Hamiltonian has the form [S3]

$$\hat{\mathcal{H}}_{\text{hf}} = 2\mu_B\mu_I \left[\frac{8\pi}{3}\hat{s}\delta(r) + \frac{\hat{l}}{r^3} - \frac{\hat{s}}{r^3} + 3\frac{r(\hat{s}\cdot r)}{r^5} \right], \quad (\text{S3})$$

where μ_B is the Bohr magneton, μ_I is the nuclear magnetic moment, I is the nuclear spin, $\hat{l} = -i[r \times \nabla]$ is the angular momentum operator, and s is the electron spin. The origin of the coordinate frame is chosen at the nucleus. The first term in Eq. (S3) describes contact interaction, while the others stand for the dipole-dipole interaction.

To calculate the hyperfine coupling constants we apply the method introduced in Ref. S4 and developed in Refs. S5 and S6. The bulk AlAs is described by the T_d point symmetry group with the minimum of the conduction band in the vicinity of X point of the Brillouin zone [S7]. The local symmetry in this valley is reduced and the symmetry group of the K_X Bloch wave vector is D_{2d} .

The irreducible representation of the electron wave function depends on the choice of the central point. Provided it is placed at the As atom the corresponding representation is X_6 [S8]. However as soon as the symmetry center is placed at the Al atom in the same elementary cell the representation is changed to X_7 . Indeed every new symmetry operation can be presented as the old point symmetry operation plus the translation by the vector τ . In the K_X point of the Brillouin zone such translation is equivalent to the multiplication by the factor $e^{iK_X\tau} = \pm 1$. This factor belongs to X_4 representation of D_{2d} group. Therefore when the central point is chosen at Al atom the wave function transforms according to $X_6 \otimes X_4 = X_7$ representation [S8].

The tight-binding calculations show that for the central point chosen at As atom the dominant contribution to the orbital part of the wave function belongs to X_1 representation [S9]. To be specific we consider the electron wave function in the X valley oriented along z direction; the wave functions in the two other valleys can be obtained by rotation of the coordinate frame. We decompose the orbital part of the wave function in the vicinity of each nucleus into the s , p and d shells as

$$\Psi_{\text{As}} = \alpha_S S(\theta, \phi) R_s(r) + \alpha_D D_{z^2}(\theta, \phi) R_d(r), \quad (\text{S4a})$$

$$\Psi_{\text{Al}} = \alpha_P P_z(\theta, \phi) R_p(r) + \alpha_T D_{xy}(\theta, \phi) R_d(r). \quad (\text{S4b})$$

Here α_l ($l = S, P, T, D$) are the coefficients, the functions $R_{s,p,d}(r)$ are the radial parts of the corresponding atomic orbitals, and the angular dependencies are described by the tesseral harmonics S for s shell, P_x, P_y, P_z for p orbitals and $D_{xy}, D_{yz}, D_{xz}, D_{x^2-y^2}, D_{z^2}$ for d orbitals [S10]. Note that hereafter we neglect the electron Bloch wave vector [S4] as well as the corrections related to the size quantization.

Calculation of the hyperfine interaction, Eq. (S3), for the functions in the form of Eq. (S4) yields

$$H_{\text{hf}} = A^\perp (I_x s_x + I_y s_y) + A^\parallel I_z s_z, \quad (\text{S5})$$

where

$$A^i = \frac{4}{3} \mu_B \mu_I R_s^2(0) \sum_l |\alpha_l|^2 C_l^i M_l. \quad (\text{S6})$$

Here $i = \perp, \parallel$ and the coefficients C_l^i are given in Tab. S1. The numbers M_l describe the relative strengths of the corresponding contributions to the hyperfine interaction. By definition $M_S = 1$, while for $l = P$ and $l = T, D$

$$M_l = \frac{1}{R_s^2(0)} \int_0^\infty \frac{R_{p,d}^2(r)}{r} dr, \quad (\text{S7})$$

TABLE S1. The parameters C_l^i of the hyperfine interaction constants, Eq. (S6).

C_l^i	$l = S$	$l = P$	$l = T$	$l = D$
$i = \perp$	1	-3/5	3/7	-3/7
$i = \parallel$	1	6/5	-6/7	6/7

TABLE S2. The parameters M_l of the hyperfine interaction constants, Eq. (S6), calculated using the hydrogen-like wave functions.

	M_S	M_P	$M_T = M_D$
Al	1	0.08024	0.01605
Ga	1	0.05671	0.3849
As	1	0.04815	0.2898

respectively, and we have disregarded the crosscorrelations between different l .

Calculation of M_l can be explicitly done for the particular model of radial functions. We consider the hydrogen like functions and the results of our calculations are presented in Tab. S2. The orbital exponents for these functions were calculated in Ref. S11 using the self-consistent-field function. We note that one can also use Slater functions with the parameters determined by Slater rules [S12] or from the *ab-initio* calculations [S13].

Finally the probabilities of the atomic shell occupations, $|\alpha_l|^2$ multiplied by the probability to occupy the particular atom, were calculated in the WIEN2k package [S9 and S14] using modified Becke-Johnson (mBJ) exchange-correlation potential [S15]. The results are presented in Tab. S3. One can note that these values somewhat differ from the accepted ones [S16], but the main features are generally the same.

The hyperfine interaction constants can now be calculated after Eq. (S6) and the results are presented in Tab. S4. The hyperfine constants are given in the arbitrary units, because the manybody effects considerably

TABLE S3. The contributions of atomic shells to the electron density, $|\alpha_l|^2$ multiplied by the probabilities to be in the given sublattice.

		S	P	T	D
GaAs	Ga	0.507			
	As	0.493			
AlAs	Al		0.263	0.087	
	As	0.252			0.398

TABLE S4. The hyperfine coupling constants calculated after Eq. (S6). The values are given in the arbitrary units.

		cation	anion
GaAs	$A^\perp = A^\parallel$	3.12	3.97
AlAs	A^\perp	-0.03	1.63
	A^\parallel	0.07	2.82

modify electron wavefunction in the vicinity of the nuclei and the outlined approach allows only for the reliable calculation of the hyperfine coupling constants relative values [S6 and S17]. The hyperfine constants given in Tab. S4 in the arbitrary units allow one to estimate the absolute values of the coupling constants comparing the results obtained for AlAs and GaAs conduction bands. Since the conduction band minimum in GaAs is formed only by s orbitals the Eqs. (S3)–(S6) the experiment can be equally applied to the Γ point of GaAs Brillouin zone. Note that in the considered AlAs QW the electrons occupy the in-plane X valleys, therefore the experimentally observed A_{zz} in the notations of the main text is given by A^\perp . Assuming that the maximum Overhauser field for completely polarized arsenic nuclei is 2.76 T ($A = 47 \mu\text{eV}$) [S18 and S19] we obtain the maximum theoretical Overhauser field in AlAs 250 mT.

The contribution to the Overhauser field from the Al nuclei is very small because this contribution is related mainly to the p shell, which is characterized by small M_P . The corresponding hyperfine interaction is strongly anisotropic, as described by $C_P^\parallel = -2C_P^\perp$. For the Al nuclei $A^\perp = -0.4 \mu\text{eV}$ and $A^\parallel = 0.8 \mu\text{eV}$. By contrast for the arsenic atom the considerable fraction of the electron density is in the s shell and gives rise to the quite pronounced hyperfine interaction, $A^\parallel = 33 \mu\text{eV}$. The d shell of the arsenic also contributes to hyperfine coupling, and induces the anisotropy of hyperfine interaction in AlAs, which results into $A^\perp = 19 \mu\text{eV}$.

III. S3. DISCUSSION OF NUCLEAR SPIN RELAXATION MECHANISM

Nuclear spin relaxation rate strongly depends on the Landau level filling factor, which evidences the hyperfine mediated mechanism of spin relaxation. However the electron-nuclear spin flip process is accompanied by the change of electron Zeeman energy. The electron-electron exchange interaction results into the enhancement of the splitting between spin sublevels [S20]. For the Landau level filling factor $\nu = 1$ ($B = 6.36$ T) the enhanced g -factor is $g^{**} \approx 9$ [S21] and the corresponding spin splitting is $\Delta E = 3.3$ meV. On the other hand the temperature expressed in energy units is $k_B T = 0.13$ meV and the Landau level broadening is

$\Gamma = e\hbar\sqrt{2B/(\pi\mu m_i m_i)} = 0.12$ meV [S22]. Therefore the phonon assisted [S23] and scattering assisted [S24] electron nuclear spin flip processes are suppressed respectively by the factors $\exp(-\Delta E/k_b T)$ and $\exp(-\Delta E/\Gamma)$ of the order of $10^{-12} \div 10^{-13}$. In the similar experiments in GaAs [S24] the suppression is much weaker $\exp(-\Delta E/\Gamma) \sim 10^{-5}$ mainly because of the smaller effective mass. In the same time the nuclear spin relaxation rate in this structure is only 12 times faster than in AlAs structure under study. This suggests that the nuclear spin relaxation can be caused by the processes that do not involve real electron spin transitions.

The nuclear spin diffusion is caused by the dipole-dipole interaction between nuclear spins [S3]. The strength of this interaction is very small $H_{dd} \sim 10^{-11}$ meV, while the Knight field experienced by the nuclei at $\nu = 1$ can be estimated as $K \sim A_{zz}\Omega n/l \sim 10^{-7}$ meV, where $\Omega = 0.045$ nm³ is the elementary cell

volume and $l = 16$ nm is the QW width. The Knight field acts as an additional magnetic field, therefore the gradient of the Knight field along the growth axis related to the electron envelope wave function blocks nuclear spin diffusion. The energy barrier for the two nearest nuclei spins flip-flop process is of the order of $\Delta K \sim K a_0/l \approx 4 \cdot 10^{-9}$ meV, where a_0 is the GaAs lattice constant. As a possible mechanism of nuclear spin relaxation we propose nuclear spin diffusion by electron assisted RKKY interaction [S25]. This process does not involve real electron spin transitions, and the energy difference between initial and final states can be easily compensated by the electron scattering because $\Gamma \gg \Delta K$. However the microscopic theory of this effect is beyond the scope of this paper and will be reported elsewhere. We note that the other mechanisms related to the spin-orbit coupling [S26] or collective excitations [S27] might also contribute to nuclear spin relaxation.

-
- [S1] R. I. Dzhioev and V. L. Korenev, Phys. Rev. Lett. **99**, 037401 (2007).
- [S2] R. K. Sundfors, R. K. Tsui, and C. Schwab, Phys. Rev. B **13**, 4504 (1976).
- [S3] A. Abragam. *The principles of Nuclear Magnetism*. Oxford University Press, London, 1961.
- [S4] E. I. Gryncharova and V. I. Perel, Semiconductors **11**, 997 (1977).
- [S5] J. Fischer, W. A. Coish, D. V. Bulaev, and D. Loss, Phys. Rev. B **78**, 155329 (2008).
- [S6] E. Chekhovich, M. Glazov, A. Krysa, M. Hopkinson, P. Senellart, A. Lemaitre, M. Skolnick, and A. Tartakovskii, Nature Physics **9**, 74 (2013).
- [S7] I. Vurgaftman, J. R. Meyer, and L. R. Ram-Mohan, J. Appl. Phys. **89**, 5815 (2001).
- [S8] G. L. Bir and G. E. Pikus, *Symmetry and Deformation Effects in Semiconductors* (Nauka, Moscow, 1972).
- [S9] M. O. Nestoklon private communication.
- [S10] D. A. Varshalovich, A. N. Moskalev, and V. K. Khersonskii. *Quantum theory of angular momentum*. World Scientific Pub., 1988.
- [S11] E. T. Clementi and D. L. Raimondi. Atomic screening constants from SCF functions. J. Chem. Phys. **38**, 2686 (1963).
- [S12] J. C. Slater, Phys. Rev. **36**, 57 (1930).
- [S13] R. Benchamekh, F. Raouafi, J. Even, F. Ben Cheikh Larbi, P. Voisin, and J.-M. Jancu, Phys. Rev. B **91**, 045118 (2015).
- [S14] P. Blaha, K. Schwarz, G. Madsen, D. Kvaniscka, and J. Luitz, *Wien2k, An Augmented Plane Wave Plus Local Orbitals Program for Calculating Crystal Properties* (Vienna University of Technology, Vienna, 2001).
- [S15] F. Tran and P. Blaha, Phys. Rev. Lett. **102**, 226401 (2009).
- [S16] P. Boguslawski and I. Gorczyca, Semicond. sci. tech. **9**, 2169 (1994).
- [S17] M. Vidal, M. V. Durnev, L. Bouet, T. Amand, M. M. Glazov, E. L. Ivchenko, P. Zhou, G. Wang, T. Mano, T. Kuroda, X. Marie, K. Sakoda, and B. Urbaszek, Phys. Rev. B **94**, 121302(R) (2016).
- [S18] D. Paget, G. Lampel, B. Sapoval, and V. I. Safarov, Phys. Rev. B **15**, 5780 (1977).
- [S19] B. Urbaszek, X. Marie, T. Amand, O. Krebs, P. Voisin, P. Maletinsky, A. Högele, and A. Imamoglu, Rev. Mod. Phys. **85**, 79 (2013).
- [S20] T. Ando, A. B. Fowler, and F. Stern, Rev. Mod. Phys. **54**, 437 (1982).
- [S21] S. J. Papadakis, E. P. De Poortere, and M. Shayegan, Phys. Rev. B **59**, R12743 (1999).
- [S22] D. Weiss and K. v. Klitzing, in *High Magnetic Fields in Semiconductor Physics*, edited by G. Landwehr, Springer Series in Solid State Sciences Vol. 71 (Springer-Verlag, Berlin, 1987), p. 57.
- [S23] J. H. Kim, I. D. Vagner, and L. Xing, Phys. Rev. B **49**, 16777 (1994).
- [S24] A. Berg, M. Dobers, P. R. Gerhardtts, and K. von Klitzing, Phys. Rev. Lett. **64**, 2563 (1990).
- [S25] C. Latta, A. Srivastava, A. Imamoglu, Phys. Rev. Lett. **107**, 167401 (2011).
- [S26] K. Hashimoto, K. Muraki, N. Kumada, T. Saku, and Y. Hirayama, Phys. Rev. Lett. **94**, 146601 (2005).
- [S27] R. Côté, A. H. MacDonald, L. Brey, H. A. Fertig, S. M. Girvin, H. T. C. Stoof, Phys. Rev. Lett. **78**, 4825 (1997).